Improvement in the Luminescence Properties and Processability of LaF_3/Ln and $LaPO_4$/Ln Nanoparticles by Surface Modification

Jan W. Stouwdam† and Frank C. J. M. van Veggel*,†

Laboratories of Supramolecular Chemistry and Technology & MESA+ Research Institute, University of Twente, P.O. Box 217, 7500 AE Enschede, The Netherlands

Received June 30, 2004

The surface of lanthanide(III)-doped $LaPO_4$ nanoparticles was modified by reaction with an alcohol, leading to a covalent bond between the ligand and the particle surface. The surface of lanthanide(III)-doped LaF_3 nanoparticles was modified to alter the solubility of the nanoparticles and study the influence of surface effects on the luminescence of lanthanide ions doped in the nanoparticles. The coordinated organic ligands can be modified by a quantitative exchange reaction in solution or by using functionalized ligands during the synthesis. Variation of the ratio of ligand to core reagents had a significant influence on the size of the nanoparticles. Smaller nanoparticles were formed with a higher ligand ratio. The optical properties of these nanoparticles show a strong dependence on nanoparticle size, indicating the influence of quenching probably by CH and OH groups at or near the surface of the nanoparticle cores. The luminescence lifetime of LaF_3/Eu nanoparticles varied from 6.5 to 7.4 ms for nanoparticles with an average size of 7.1 to 8.4 nm. A significant reduction of the quenching from the surface of the nanoparticles was obtained by the synthesis of core−shell nanoparticles, in which a shell of LaF_3 was grown epitaxially around the doped core nanoparticles. This leads to an increase in the luminescence lifetime of the Eu^{3+} ion and the observation of emissions from the $^5D_2$ energy level, in addition to emissions from the $^5D_1$ and $^5D_0$ levels. The quantum yield of LaF_3/Ce,Tb nanoparticles could be increased from 24 to 54% by the growth of a LaF_3 shell around the nanoparticles.

Introduction

The luminescence of lanthanide ions in organic materials can greatly be improved by doping them in the inorganic core of nanoparticles that are soluble in organic solvents.[1,2] Ligands that are coordinated to the surface of the nanoparticles prevent the particles from clustering and also determine the solubility of the nanoparticles. An important tool in the processing of these nanoparticles is the control over the surface-bound ligands, because in this way the solubility of the nanoparticles can be tuned. The luminescence of lanthanide ions doped in nanoparticles shows properties similar to those of the lanthanide ions doped in the corresponding bulk materials, because the symmetry around the lanthanide ions is the same.[3] However, quenching of lanthanide ions close to the surface of the nanoparticles causes a multiexponential decay of the luminescence of the lanthanide ions.[4−6] The quenching by surface-bound organic groups and coordinated water should be reduced by the synthesis of core−shell nanoparticles in which the core is doped with the luminescent lanthanide ions and the shell is not. In this structure the distance between the luminescent lanthanide ions and the surface quenchers is increased, thus, reducing the nonradiative pathways.

The synthesis of core−shell nanoparticles has been applied successfully to semiconductor nanoparticles of CdSe[7−9] and InAs.[10] The reduction of quenching by surface-coordinated impurities increased the quantum yield of these nanoparticles from a few percent to up to 80%.

Recently, Haase et al. reported the synthesis of core−shell nanoparticles of a $CePO_4$/Tb core covered with a $LaPO_4$ shell.[11] An increase in the quantum yield of these nanoparticles, from 53% for the core particles to 80% for the core−shell particles, was observed.

The successful synthesis of core−shell nanoparticles involves the growth of an undoped shell around a doped core. A good control over the particle size during the synthesis is, therefore, required. Recently, we reported the synthesis of LaF_3 nanoparticles doped with luminescent lanthanide ions emitting in the visible and near-infrared.[1,4] This material has low phonon energies and is, therefore, well suited for the emission of lanthanide ions in the near-infrared.[12] The luminescence of the lanthanide ions doped in these nanoparticles showed a multiexponential decay, which was ascribed to quenching from outside the nanoparticles. In this paper, the surface of these nanoparticles was modified to control the solubility and to improve the luminescence properties by the synthesis of core−shell nanoparticles.

Experimental Section

General Procedures. Transmission electron microscopy (TEM) images were collected on a Philips CM 30 Twin FTEM,

* To whom correspondence should be addressed. E-mail: fvv@uvic.ca.

† Current address: University of Victoria, Department of Chemistry, P.O. Box 3065, Victoria, British Columbia, Canada V8W 3V6.

(1) Stouwdam, J. W.; van Veggel, F. C. J. M. *Nano Lett.* **2002**, *2*, 733.
(2) Hebbink, G. A.; Stouwdam, J. W.; Reinhoudt, D. N.; van Veggel, F. C. J. M. *Adv. Mater.* **2002**, *14*, 1147.
(3) Haase, M.; Riwotzki, K.; Meyssamy, H.; Kornowski, A. *J. Alloys Compd.* **2000**, *303−304*, 191.
(4) Stouwdam, J. W.; Hebbink, G. A.; Huskens, J.; van Veggel, F. C. J. M. *Chem. Mater.* **2003**, *15*, 4604.
(5) Riwotsky, K.; Meyssamy, H.; Kornowski, A.; Haase, M. *J. Phys. Chem. B* **2001**, *104*, 2824.
(6) Krebs, J. K.; Feofilov, S. P.; Kaplyanskii, A. A.; Zakharchenya, R. I.; Happek, U. *J. Lumin.* **1999**, *83−84*, 209.
(7) Hines, M. A.; Guyot-Sionnest, P. *J. Phys. Chem.* **1996**, *100*, 468.
(8) Peng, X.; Schlamp, M. C.; Kadavanich, A. V.; Alivisatos, A. P. *J. Am. Chem. Soc.* **1997**, *119*, 7019.
(9) Danek, M.; Jensen, K. F.; Murray, C. B.; Bawendi, M. G. *Chem. Mater.* **1996**, *8*, 173.
(10) Cao, Y.; Banin, U. *J. Am. Chem. Soc.* **2000**, *122*, 9692.
(11) Kömpe, K.; Borchert, H.; Storz, J.; Lobo, A.; Adam, S.; Möller, T.; Haase, M. *Angew. Chem., Int. Ed.* **2003**, *42*, 5513.
(12) Weber, M. J. *Phys. Rev. B* **1967**, *157*, 262.

10.1021/la048379g CCC: $27.50 © 2004 American Chemical Society
Published on Web 11/16/2004

operating at 300 kV. Samples were prepared by evaporating a drop of a diluted nanoparticle dispersion in dichloromethane on a carbon-coated 200 mesh copper grid. Size distributions were determined by measuring the sizes of at least 100 nanoparticles from different places on the grid. Melting points were determined with a Reichert melting point apparatus and are uncorrected. Mass spectra were recorded on a Finnigan MAT 90 spectrometer using nitrobenzyl alcohol as a matrix or on a Perkin-Elmer/Perspective biosystems Voyager-DE-RP matrix-assisted laser desorption ionization time-of-flight (MALDI-TOF) mass spectrometer. ^{1}H NMR spectra were recorded with a Varian-300 spectrometer using $CDCl_3$ as the solvent unless stated otherwise, using residual $CHCl_3$ ($\delta = 7.26$ ppm) as the internal standard. ^{1}H NMR measurements on nanoparticles were performed on undoped nanoparticles to exclude the influence of the magnetic moment of some of the luminescent lanthanide ions. Luminescence measurements were performed as described before.[4]

The lanthanide salts were purchased from Aldrich or Acros in the highest purity available (at least 99.9%). Octadecanol (99%), sodium fluoride (99%), oleic acid, and tris(ethylhexyl)phosphate (98%) were purchased from Fluka, phosphorus pentasulfide (99%) was purchased from Aldrich, and trioctylamine (98%) and phosphorus oxychloride were purchased from Acros. All chemicals were used as received without further purification. CH_2Cl_2 and hexane were distilled from $CaCl_2$, and ethyl acetate was distilled from K_2CO_3. Tetrahydrofuran (THF) was freshly distilled from Na/benzophenon.

Ligand 1. A total of 19.0 g (0.07 mol) of octadecanol and 4.4 g (0.02 mol) of P_2S_5 were heated at 75 °C for 3 h. The suspension was cooled to room temperature followed by the addition of 50 mL of dichloromethane. To remove inorganic salts the solution was filtered followed by evaporation of the solvent. The remaining residue was taken up in 50 mL of hexane, and ammonia was bubbled through the solution. The precipitate was separated by filtration, washed with hexane, and dried; yield 13 g, 60%, mp 103−106 °C. ^{1}H NMR (DMSO-d_6): δ 7.2−6.9 (broad, 4H), 3.7 (dt, $J = 8.1$, 6.6 Hz, 4H), 1.5−1.4 (m, 4H), 1.35−1.1 (m, 60H), 0.84 (t, $J = 6.2$ Hz, 6H). MS (MALDI-TOF) $m/z = 634.0$ [$(M - NH_4)^-$ calcd for $C_{36}H_{74}O_2PS_2$, 633.5]. Anal Calcd for $C_{36}H_{78}NO_2PS_2$: C, 66.31; H, 12.06; N, 2.15; S, 9.83. Found: C, 66.50; H, 12.24; N, 2.27; S, 9.56.

Ligand 2. A total of 20.0 g (0.08 mol) of bromoundecanol, 9.6 g (0.1 mol) of phenol, and 4.5 g (0.1mol) of K_2CO_3 were refluxed in 100 mL of acetonitril overnight under an argon atmosphere. The reaction mixture was cooled to room temperature, and 300 mL of ethyl acetate was added. The organic phase was washed three times with 1 N NaOH and dried over $MgSO_4$. The solvent was evaporated, and the residue was dried.

A total of 19.6 g (0.074 mol) of the alcohol obtained in the first step and 4.7 g (0.021 mol) of P_2S_5 were heated at 75 °C for 3 h. The suspension was cooled to room temperature followed by the addition of 50 mL of dichloromethane. To remove inorganic salts the solution was filtered and the solvent was evaporated. The remaining residue was taken up in 50 mL of hexane, and ammonia was bubbled through the solution. The precipitate was separated by filtration, washed with hexane, and dried; yield 19.8 g, 78%, mp 80−82 °C. ^{1}H NMR (acetone-d_6): δ 7.8−7.5 (broad, 4H), 7.3 (m, 4H), 6.9 (m, 6H), 4.0 (t, $J = 6.6$ Hz, 4 H), 3.9 (dt, $J = 8.1$, 6.6 Hz, 4H), 1.8 (m, 4H), 1.6 (m, 32H). MS (FAB) $m/z = 621.1$ [$(M - NH_4)^-$ calcd for $C_{34}H_{54}O_4PS_2$, 621.3]. Anal Calcd for $C_{34}H_{58}NO_4PS_2$: C, 63.81; H, 9.14; N, 2.19; S, 10.02. Found: C, 63.87; H, 9.04; N, 2.23; S, 10.07.

Ligand 3. A mixture of 10.0 g (39 mmol) of bromoundecanol, 7.8 g (51 mmol) of methyl-4-hydroxy benzoate, and 7.1 g (51 mmol) of K_2CO_3 in 100 mL of acetonitril was refluxed overnight. The mixture was cooled to room temperature, and 300 mL of ethyl acetate was added. This solution was washed with 1 N NaOH three times and one time with water. The organic layer was dried over $MgSO_4$ and filtered, and the organic solvent was removed under a vacuum.

A total of 9.7 g (30 mmol) of the alcohol obtained in the first step was heated with 1.9 g (8.6 mmol) of P_2S_5 at 80 °C for 3 h. The suspension was cooled to room temperature followed by the addition of 50 mL of dichloromethane. To remove inorganic salts the solution was filtered and the solvent was evaporated. The remaining residue was taken up in 50 mL of toluene/hexane, and ammonia was bubbled through the solution. The precipitate was separated by filtration, washed with hexane, and dried. The product was obtained as a white solid; yield 73%, mp 81−83 °C. ^{1}H NMR (acetone-d_6): δ 7.9 (d, $J = 9.2$ Hz, 4H), 7.0 (d, $J = 9.2$ Hz, 4H), 4.1 (t, $J = 6.6$ Hz, 4H), 3.9 (dt, $J = 8.4$, 6.6 Hz, 4H), 3.8 (s, 6H), 1.8 (m, 4H), 1.5−1.3 (m, 32H). MS (FAB) $m/z = 737.5$ [$(M - NH_4)^-$ calcd for $C_{38}H_{58}O_8PS_2$, 737.0]. Anal Calcd for $C_{38}H_{62}O_8PS_2N$: C, 60.37; H, 8.27; N, 1.85; S, 8.48. Found: C, 59.87; H, 8.72; N, 1.95; S, 8.37.

Ligand 4. A mixture of 7.1 g (51 mmol) of K_2CO_3, 6.6 g (51 mmol) of 4-chlorophenol, and 10.0 g (39 mmol) of bromoundecanol in 100 mL of acetonitril was refluxed overnight. The mixture was cooled to room temperature, and 300 mL of ethyl acetate were added. This solution was washed with 1 N NaOH three times and one time with water. The organic layer was dried over $MgSO_4$ and filtered, and the organic solvent was removed under a vacuum.

A total of 9.7 g (32.5 mmol) of the alcohol obtained in the first step was heated with 2.1 g (9.3 mmol) of P_2S_5 at 80 °C for 3 h. The suspension was cooled to room temperature followed by the addition of 50 mL of dichloromethane. To remove inorganic salts the solution was filtered and the solvent was evaporated. The remaining residue was taken up in 50 mL of hexane, and ammonia was bubbled through the solution. The precipitate was separated by filtration, washed with hexane, and dried. The product was a white solid obtained in 70% yield, mp 57−60 °C. ^{1}H NMR ($CDCl_3$): δ 7.2 (d, $J = 9.2$ Hz, 4H), 6.8 (d, $J = 8.8$ Hz, 4H), 4.0 (dt, $J = 8.4$, 6.9 Hz, 4H), 3.9 (t, $J = 6.6$ Hz, 4H), 1.8−1.7 (m, 8H), 1.4−1.3 (m, 28H). MS (FAB) $m/z = 689.2$ [$(M - NH_4)^-$ calcd for $C_{34}H_{52}O_4PS_2Cl_2$, 689.2]. Anal Calcd for $C_{34}H_{56}O_4PS_2NCl_2$: C, 57.61; H, 7.96; N, 1.98; S, 9.05. Found: C, 57.42; H, 8.05; N, 2.04; S, 9.20.

Ligand 5. A solution of 5.0 g (18.5 mmol) of octadecanol in 20 mL of anhydrous THF was slowly dropped into 1.4 g (9.2 mmol) of $OPCl_3$ at −15 °C under Ar. The solution was slowly allowed to warm to room temperature and stirred for 2 h. After the addition of 1 mL of water, the solution was vigorously stirred for 1 h, followed by the addition of 100 mL of ethyl acetate. The organic phase was separated and washed three times with 1 N HCl. The organic layer was dried over $MgSO_4$ and evaporated to dryness. The residue was dissolved in 20 mL of hexane, and NH_3 was bubbled to the solution. The precipitate was filtered, washed with hexane, and dried. To substitute the ammonium counterion for a proton, the product was taken up in ethyl acetate and washed three times with 1 N HCl. The organic layer was dried over $MgSO_4$ and evaporated to dryness. A white solid remained; yield 2.9 g, 53%, mp 71−73 °C. ^{1}H NMR ($CDCl_3$): δ 4.1 (dt, $J = 7.0$, 6.6 Hz, 4H), 1.7 (m, 4H), 1.3 (m, 60H), 0.9 (t, $J = 6.6$ Hz, 6H). MS (FAB) $m/z = 602.5$ [(M^+) calcd for $C_{36}H_{75}O_4P$, 603.0]. Anal Calcd for $C_{36}H_{75}O_4P$: C, 71.71; H, 12.54. Found: C, 71.45; H, 12.80.

LaF_3 Nanoparticles. The LaF_3 nanoparticles were prepared by heating a solution of 0.95 mmol of the ligand and 126 mg (1.0 mmol) of NaF in 35 mL of ethanol/water at 75 °C. A solution of $La(NO_3)_3 \cdot 6H_2O$ and $Eu(NO_3)_3 \cdot 6H_2O$ (1.3 mmol total) in 2 mL of water was added dropwise, and the solution was stirred at 75 °C for 2 h and then cooled to room temperature. The precipitate was separated by centrifugation and was washed subsequently with water and ethanol. The nanoparticles were further purified by dispersing in 2 mL of dichloromethane and precipitation by the addition of 15 mL of ethanol. After separation by centrifugation the nanoparticles were dried in a vacuum over P_2O_5 for 2 days. After drying the nanoparticles, they are soluble in apolar solvents such as chloroform, dichloromethane, and toluene.

Surface Modification of $LaPO_4$ Nanoparticles. The surface phosphate groups of the nanoparticles were first reacted with phosphorus oxychloride by heating 100 mg of nanoparticles in 5 mL of $OPCl_3$ for 2 h at 120 °C. After 2 h the solution was cooled to room temperature and the $OPCl_3$ was evaporated under a vacuum followed by the addition of 5 mL of toluene containing 1 mL of dodecanol. This solution was refluxed for 2 h and then cooled to room temperature. To remove excess dodecanol the nanoparticles were precipitated by the addition of 20 mL of methanol and separated by centrifugation. After washing a few times with methanol the nanoparticles were soluble in an apolar solvent like toluene, dichloromethane, and chloroform.

Exchange Reaction on LaF_3 Nanoparticles. To a solution of 100 mg of LaF_3 nanoparticles in 5 mL dichloromethane was added 100 mg of ligand **5** or **6** and 100 μL of triethylamine. This solution was stirred overnight, and methanol was added to precipitate the nanoparticles. The precipitate was separated by centrifugation and washed repeatedly with polar solvents such as methanol, ethanol, or acetone, until no free ligand was observed in the ^{1}H NMR spectrum.

Core−Shell Nanoparticles. NaF was substituted by NH_4F because of an increased solubility in water. The core of the nanoparticles was synthesized by the dropwise addition of the lanthanide salts to the NH_4F and ligand **1** in 35 mL of a water/ethanol mixture at 75 °C. This mixture was stirred for 10 min followed by the shell growth. To determine the best way of growing a shell around a core, several methods were tested.

Method 1. After the synthesis of the core nanoparticles 3.0 mmol of NH_4F was added dropwise followed by the dropwise addition of 1.3 mmol of $La(NO_3)_3$.

Method 2. The synthesis of the core nanoparticles was started with 6.0 mmol of NH_4F, and to this solution was first added the lanthanide salts for the core, followed after 10 min by the addition of $La(NO_3)_3$ for the shell.

Method 3. After the synthesis of the core, 3.0 mmol of NH_4F and 1.3 mmol of $La(NO_3)_3$ dissolved in 2 mL of water were added alternately in 10 portions.

After the addition of the shell material the solution was stirred for additional 2 h at 75 °C, after which it was cooled to room temperature. The workup of the nanoparticle product was the same as for the normal LaF_3 nanoparticles.

Results and Discussion

Control of the Solubility. The surface of $LaPO_4$ nanoparticles consists of phosphate groups and some bound ethylhexyl chains left after the synthesis of the nanoparticles. These ethylhexyl chains were detected using ^{1}H NMR spectroscopy. The surface of the nanoparticles is covered with OH groups of the phosphate groups, which provide the opportunity to link covalently organic ligands to the surface. The presence of the OH groups was proven by solubility experiments. Directly after the synthesis, the nanoparticles were soluble in polar aprotic solvents, like dimethylformamide (DMF) and dimethyl sulfoxide (DMSO). This means that the surface has a polar nature, which is inconsistent with a full coverage with ethylhexyl chains of the coordinating solvent. A full coverage with these apolar ligands should make the nanoparticles soluble in apolar solvents, like hexane, toluene, and dichloromethane. The nanoparticles can be solubilized in alcohols, such as methanol and 2-propanol, by the addition of tetraalkylammonium hydroxides. The addition of tetraalkylammonium bromides does not lead to solubility in the alcohols, proving that the base is necessary to deprotonate the surface OH groups. Deprotonation of the surface OH groups leads to a negatively charged surface, which makes the coordination of the positively charged ammonium ions possible. Surface functionalization could involve the reaction of the surface OH groups with alcohols, to form phosphate esters. This would give a covalent attachment of the ligands to the nanoparticle surface in contrast to the method reported by Haase et al. in which they form a coordinative bond.[11] The OH groups of the surface phosphate groups were converted into chlorides by a reaction with phosphorus oxychloride. The surface of the nanoparticles can subsequently be functionalized by a reaction with an excess of dodecanol. The ^{1}H NMR of this product is shown in Figure 1.

The ^{1}H NMR signals of the dodecane chains are broadened as a result of the binding to the nanoparticles surface. This broadening of the NMR signals of nanoparticle-bound ligands can be ascribed to the inhomogeneous distribution of the magnetic environment around the nanoparticle and a reduction in rotational freedom of the ligand.[13,14] The shift of the CH_2O group from 3.6 ppm for dodecanol in chloroform-d_1 to 4.0 ppm confirms the covalent bonding to the particle surface. The $LaPO_4$ nanoparticles before surface functionalization were only soluble in polar aprotic solvents such as DMSO and DMF, but after the surface modification the nanoparticles are soluble in apolar solvents such as toluene, chloroform, and dichloromethane. The reaction of phosphorus oxychloride with the nanoparticles is a rigorous method to introduce reactive chlorides on the surface of the nanoparticles, and, thus, further characterization was performed to ensure that the particle cores were not changed. TEM pictures of the reaction product showed that the nanoparticle cores are still intact and that no change in nanoparticle size and size distribution had occurred (not shown). Elemental analysis confirmed the presence of about 10% organic material in the product, which is consistent with a monolayer formation around ~5-nm-sized nanoparticles. Luminescence studies also revealed no change in the environment of the Eu^{3+} ion when the surface modification was performed on Eu^{3+}-doped nanoparticles as shown in Figure 2. The luminescence spectra have the same line positions and the same peak splitting showing that the Eu^{3+} ion is still in the $LaPO_4$ matrix.

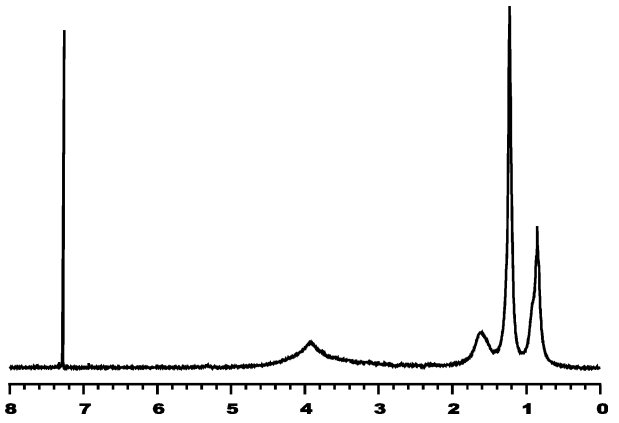

Figure 1. ^{1}H NMR of $LaPO_4$, surface-modified by a reaction with dodecanol.

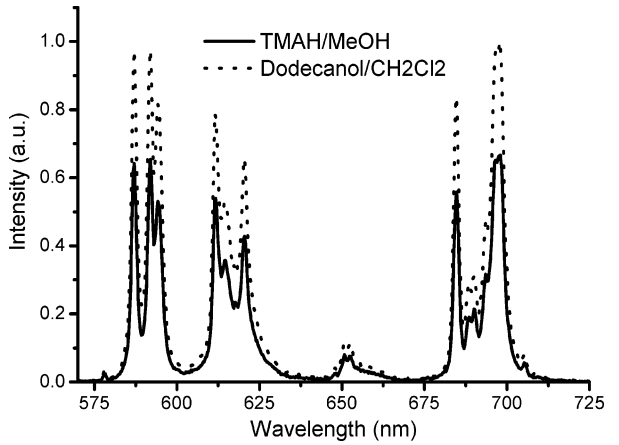

Figure 2. Emission spectra of $LaPO_4$/Eu nanoparticles in methanol with tetramethylammonium hydroxide (TMAH) and after the surface reaction with dodecanol. The difference in intensity is for clarity.

(13) Kuno, M.; Lee, J. K.; Dabbousi, B. O.; Mikulec, F. V.; Bawendi, M. G. *J. Chem. Phys.* **1997**, *106*, 9869.
(14) Sachleben, J. R.; Wooten, E. W.; Emsley, L.; Pines, A.; Colvin, V. L.; Alivisatos, A. P. *Chem. Phys. Lett.* **1992**, *198*, 431.

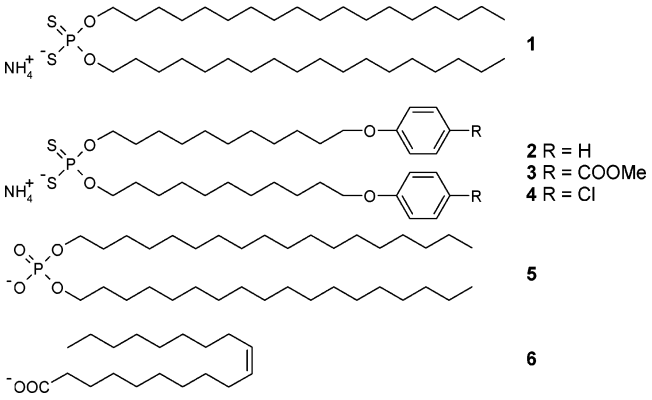

Figure 3. Ligands used in the synthesis and for the exchange of ligands on the LaF_3 nanoparticles.

The LaF_3 nanoparticles were originally synthesized with ligand **1** of Figure 3,[1] but other functionalized ligands **2**−**4** shown in Figure 3 could also be used in the synthesis, yielding nanoparticles with a different solubility.

These ligands have a dithiophosphate headgroup that binds weakly to the nanoparticle surface, to allow the growth of the nanoparticles, but coordinates strongly enough to prevent aggregation of the nanoparticles. The functionalized ligands can be synthesized in a similar manner, and all functionalized phenols that do not interfere in the second step of the reaction can be used, making this a versatile method to functionalize the surface of the LaF_3 nanoparticles. Nanoparticles synthesized with these ligands show different solubilities. Nanoparticles synthesized with ligand **2** are soluble in apolar solvents like toluene, dichloromethane, and chloroform. Nanoparticles synthesized with ligand **3** are soluble in solvents containing ester and ketone groups like ethyl acetate, cyclopentanone, and γ-butyrolactone. The latter two solvents are commonly used for the spin-coating of polymer solutions. The optical properties of the nanoparticles are independent of the functionalities of the ligand, so the functionalities do not interfere in the formation of the inorganic core of the nanoparticles. No differences in the luminescence spectrum and the luminescence lifetimes were observed, and no change in the nanoparticle cores was observed with TEM (Figure S1, Supporting Information).

Ligand exchange is another method to change the coordinated ligands around the nanoparticles. Oxygen-bearing coordinating groups have a higher binding affinity toward lanthanide ions, and examples of such ligands are dioctadecyl phosphate and oleate (ligands **5** and **6**) in Figure 3, with a phosphate group or a carboxylate group, respectively. The ligands used in the synthesis were exchanged by stirring a nanoparticle solution with ligand **5** or **6** and a small amount of base to ensure the deprotonation of the coordinating group. The exchange reaction of these ligands on the nanoparticles was monitored using ^{1}H NMR spectroscopy. Figure 4 shows the result of nanoparticles synthesized with ligand **2** and exchanged by the phosphate ligand **5**.

The ^{1}H NMR spectrum of the nanoparticles obtained after the synthesis shows broadened signals of the ligand due to coordination of the ligand to the nanoparticle surface. No free ligand is present, because no sharp signals are observed for unbound ligand in solution. A complete exchange of the dithiophoshate ligand was accomplished as can be seen in the ^{1}H NMR spectrum of the exchanged product. The aromatic proton signals at 6.8 and 7.2 ppm of the dithiophosphate ligand **2** have disappeared, and

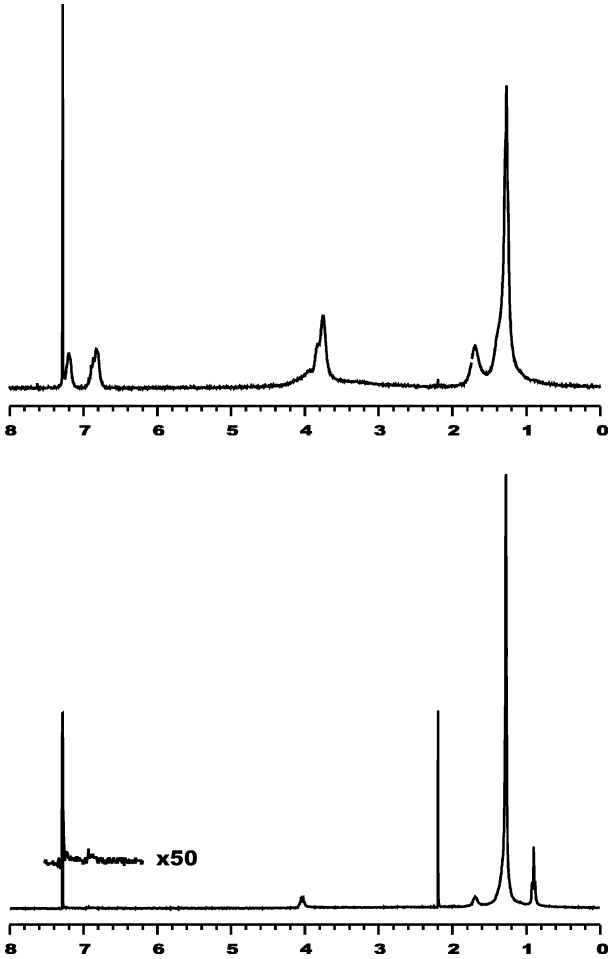

Figure 4. ^{1}H NMR spectra of LaF_3 nanoparticles synthesized with ligand **2** (top) and after exchange with ligand **5** (bottom).

the triplet of the CH_3 endgroup of the phosphate ligand **5** is present at 0.9 ppm. The ligand exchange is accompanied by a small change in solubility. Before the exchange the nanoparticles were not soluble in apolar aliphatic solvents such as hexane or pentane, but after the exchange they were. This is a confirmation that before the exchange the surface of the nanoparticles consists of the aromatic groups of the ligand making the nanoparticles soluble in aromatic solvents such as toluene. After the exchange the surface of the nanoparticles consists of the CH_3 endgroups making the nanoparticles also soluble in hexane and pentane. Figure 5 shows the ^{1}H NMR spectrum of LaF_3 nanoparticles synthesized with ligand **1**, before and after the exchange with an excess of oleate (**6**). The ligands all contain long alkyl chains, and in the proton spectrum these are mainly located between 0.9 and 2 ppm. It is difficult to observe changes in this region of the spectrum except for changes in the intensities. Protons next to the functional groups are shifted downfield and were, therefore, used to monitor the exchange reaction.

The top spectrum in Figure 5 shows the nanoparticles with ligand **1**. The spectrum of the free ligand has a characteristic double triplet at 4.1 ppm of the protons next to the phosphorus atom (see Experimental Section), but on the nanoparticles the signal is broadened and only a single broad peak is observed. The bottom spectrum shows the broadened signals of the oleate ligand coordinated to the surface of the nanoparticles after the exchange reaction. The exchange is complete, because the signal of ligand **1** at 4.1 ppm is absent and a peak of oleate at 5.2 ppm of the protons on the double bond is observed. These

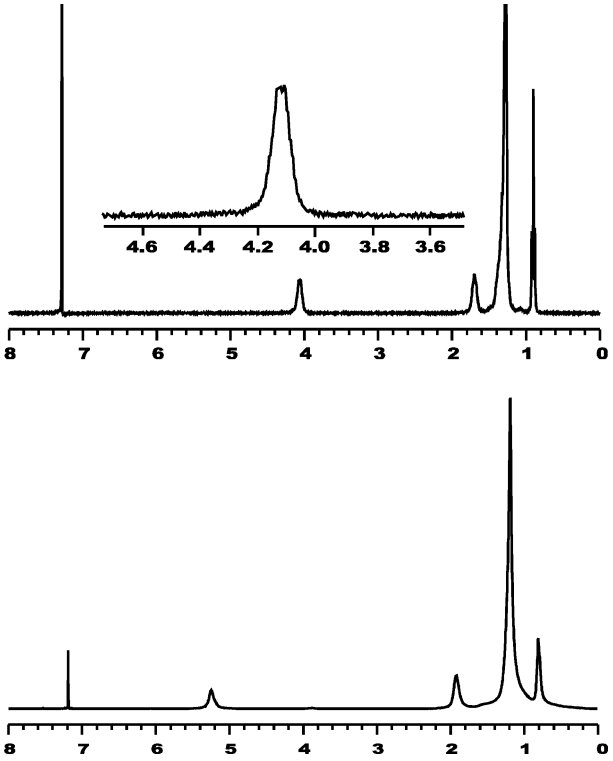

Figure 5. ^{1}H NMR spectrum of LaF_3 nanoparticles synthesized with ligand **1** before (top) and after (bottom) the exchange with ligand **6**. The inset picture shows an enlargement of the broad peak of the protons next to the dithiophosphate group.

results confirm that the ligand used in the synthesis of LaF_3 nanoparticles can be exchanged completely for another ligand with a more strongly coordinating group. This provides a straightforward method for the introduction of functional groups at the surface of the nanoparticles. The stability of the nanoparticles was not much influenced. Apparently, the coordination of the ligand to the nanoparticle surface is not the limiting factor for the stability, but the size of the hydrocarbon tails most likely is.

Differently Sized LaF_3 Nanopartices. The luminescence of the LaF_3 nanoparticles doped with luminescent lanthanide ions shows a dependence on the surface properties of the nanoparticles. The luminescence decay is multiexponential, which was attributed to surface effects.[1,4] The luminescence spectrum and the 4f energy levels of the Eu^{3+} ion are shown in Figure 6.

The Eu^{3+} ion can have several luminescent levels, depending on the phonon energy of the matrix, the doping concentration, and other quenching effects. LaF_3 has very low phonon energies in the order of 300 cm^{-1}, and in this matrix luminescence from the $^5D_0$, $^5D_1$, $^5D_2$, and $^5D_3$ levels has been observed.[15] Our LaF_3/Eu nanoparticles doped with 5% Eu^{3+} only show emission from the $^5D_0$ and $^5D_1$ levels.

Several techniques have been developed to influence the size and size distribution of nanoparticles during or after the synthesis. During the synthesis it is often a ligand that controls the growth of the nanoparticles, and changing the concentration of ligand can have an influence on the nanoparticle size.[16] When more ligand is present, there is more overall interaction between the monomer and the

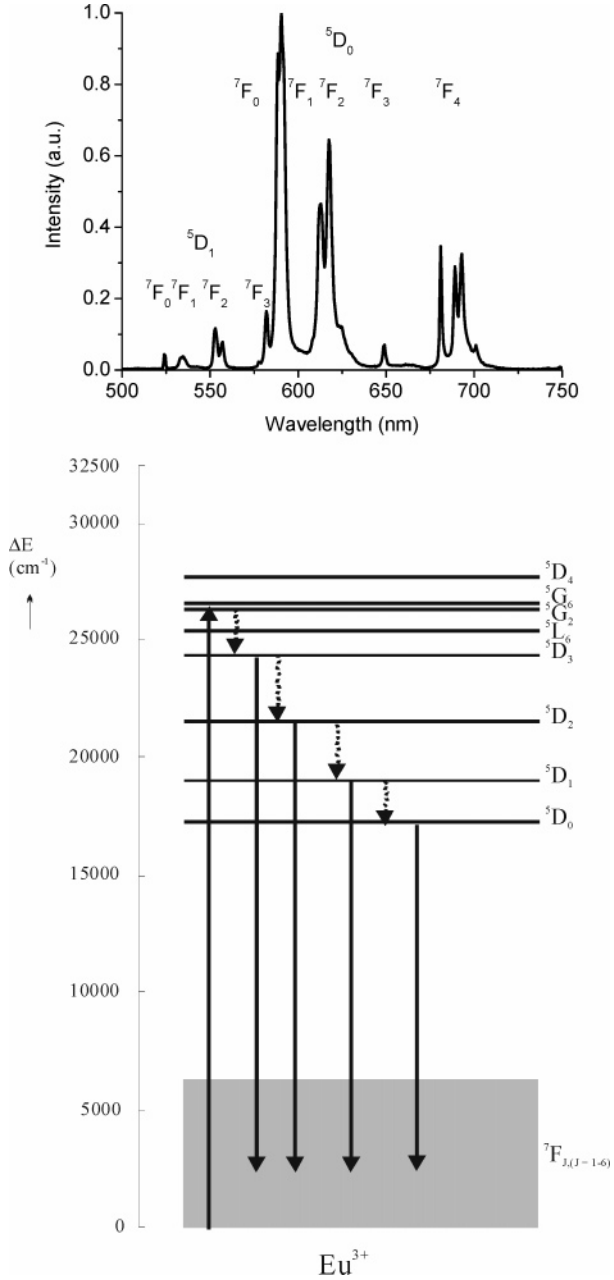

Figure 6. Luminescence spectrum (top) of LaF_3/Eu nanoparticles in dichloromethane ($\lambda_{ex} = 397$) synthesized with ligand **1**. The $^5D_0 \rightarrow {}^7F_0$ emission peak is located at 578 nm. The bottom part shows the general energy levels of the Eu^{3+} ion.

ligand, slowing down the reaction rate. This could lead to more nucleation and a decrease in nanoparticle size. The ratio of ligand to lanthanide/NaF was changed for the reaction of LaF_3/Eu nanoparticles. The influence on the size of the nanoparticles was studied with TEM. Typical TEM pictures with the corresponding size distribution histograms are shown in Figure 7.

The average sizes of the nanoparticles varied from 7.1, 7.7, and 8.4 nm for the nanoparticles synthesized with a 2:3, 1:3, and 1:6 ligand/F ratio, respectively. When the concentration of ligand was lowered, an increase in the nanoparticle size was observed. The size distributions of the nanoparticles were also increased slightly from 24, 26, and 28%, respectively. An effect on the luminescence decay was also found for nanoparticles with different sizes. The decays of the $^5D_0$ level are shown in Figure 8.

The main difference between the decays is observed shortly after the excitation pulse, where a shorter

(15) Crosswhite, H. M.; Moose, H. W. *Optical properties of ions in crystals*; Interscience: New York, 1967; p 467.
(16) Hostetler, M. J.; Wingate, J. E.; Zhong, C. J.; Harris, J. E.; Vachet, R. W.; Clark, M. R.; Londono, J. D.; Green, S. J.; Stokes, J. J.; Wignall, G. D.; Glish, G. L.; Porter, M. D.; Evans, N. D.; Murray, R. W. *Langmuir* **1998**, *14*, 17.

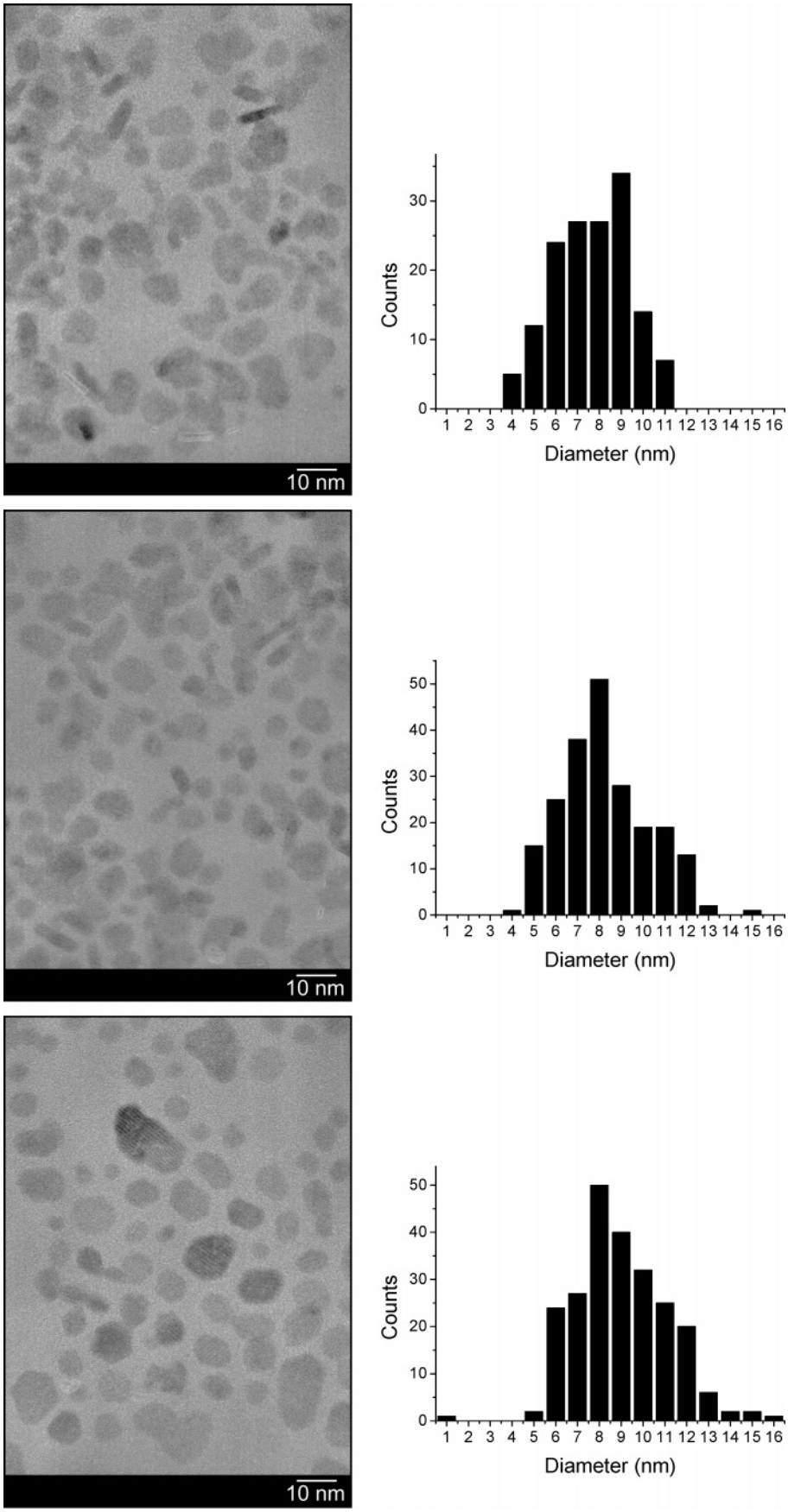

Figure 7. TEM pictures with the corresponding size distributions of LaF_3 nanoparticles synthesized with different quantities of dithio ligand.

component in the luminescence lifetime is observed for the smallest nanoparticles. This is a strong indication that the surface plays an important role in the quenching of the lanthanide ion, because the smaller nanoparticles have a larger surface-to-core ratio. About 15−20 ms after the excitation pulse the decays are almost parallel,

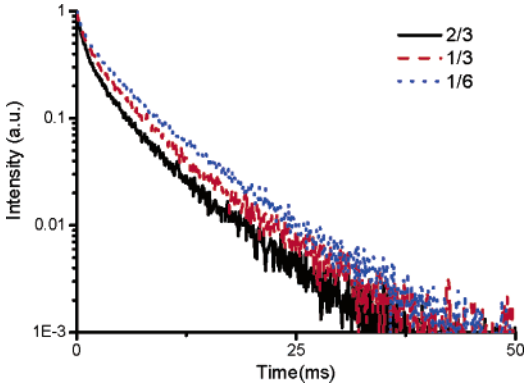

Figure 8. Luminescence decays of differently sized LaF_3/Eu nanoparticles in toluene (λ_{ex} = 397, λ_{em} = 591 nm).

indicating that the ions with a long luminescent lifetime are not much influenced by the size of the nanoparticles. The influence of surface quenching does not effectively reach to the core of the nanoparticles, so ions in the core of the small nanoparticles show the same luminescence lifetime as ions in the core of the larger nanoparticles. The luminescence lifetimes obtained after a biexponential fit are shown in Table 1. When the nanoparticle size is decreased, a clear decrease in the luminescence lifetime of both components is observed.

Table 1. Luminescence Lifetimes of the $^5D_0$ Level of Eu^{3+} (λ_{ex} = 397, λ_{em} = 591 nm) of Differently Sized LaF_3/Eu Nanoparticles after Fitting with a Biexponential Decay

average batch size (nm)	τ_1 (ms)[a,b]	τ_2 (ms)
8.4	7.4 (71%)	2.6 (29%)
7.7	6.8 (68%)	2.2 (32%)
7.1	6.5 (68%)	1.8 (32%)

[a] The percentages reflect the amount of the component contributing to the total lifetime. [b] The absolute errors are 0.2 in the lifetime and 5% in the relative amount based on duplicate measurements.

The luminescences of the $^5D_0$ level of the differently sized nanoparticles all show a multiexponential decay, indicating that surface effects play an important role in all these nanoparticle sizes. The synthesis of core−shell nanoparticles can be an easy way to enhance the luminescence properties of lanthanide-doped nanoparticles, because interaction with the high-energy vibrations of the surrounding organic environment can be reduced in this way. All the lanthanide ions involved in the lumi-

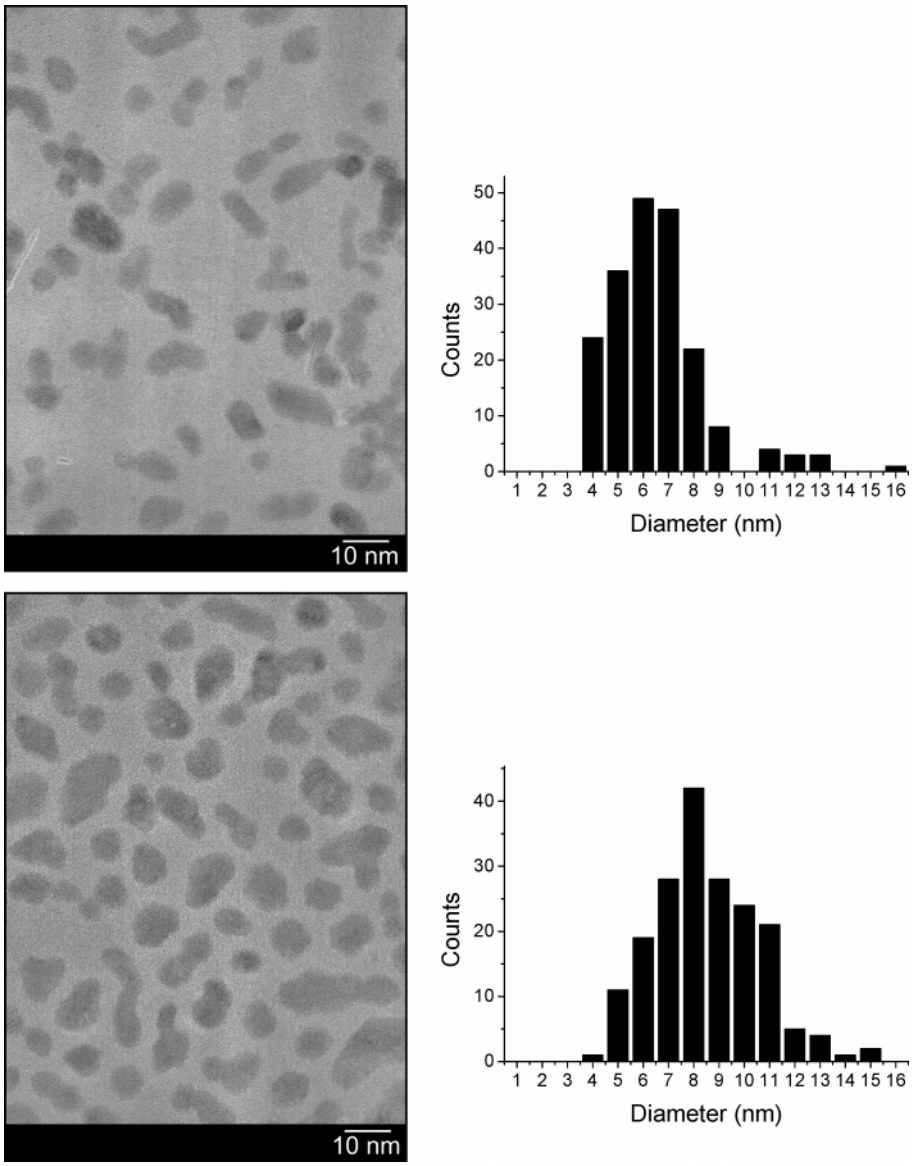

Figure 9. TEM pictures with the corresponding size distributions of core $(La_{0.4},Ce_{0.45})F_3Tb_{0.15}$ nanoparticles and core−shell $(La_{0.4},Ce_{0.45})F_3Tb_{0.15}$−$LaF_3$ nanoparticles.

nescence of the nanoparticle are doped in the core and, therefore, have no direct interaction with the surface of the nanoparticle.

Core−Shell LaF_3 Nanoparticles. The synthesis of differently sized nanoparticles by changing the ligand ratio is a strong indication that the nanoparticles form after an initial nucleation followed by growth after the addition of more reagent. This mechanism allows the growth of a core−shell structure in a one-pot synthesis, by a stepwise addition of reagents. In the core−shell experiments, ammonium fluoride was used instead of sodium fluoride as the fluoride precursor, because this salt has a higher solubility in water, making it possible to add more fluoride precursor, dissolved in a small amount of water, to the reaction mixture. Core−shell nanoparticles with a core of $(La_{0.4}Ce_{0.45})F_3Tb_{0.15}$ and a shell of LaF_3 were synthesized to study the influence of the shell on the quantum yield of the nanoparticles. During the growth of the shell no additional nucleation should occur, because this would result in the formation of undoped nanoparticles. The size of the nanoparticles is a good indication for this. The size of the nanoparticles should increase, roughly corresponding to an increase in volume that is similar to the amount of shell material added. The nanoparticle sizes before and after the growth of an undoped shell around a (La,Ce)F_3Tb core were measured using TEM. Figure 9 shows typical TEM pictures of core nanoparticles and core−shell nanoparticles, with the corresponding size distribution histograms.

A growth of the nanoparticles is clearly observed from 7.0 nm with a size distribution of 28% for the core nanoparticles to 9.0 nm with a size distribution of 23% for the core−shell nanoparticles, when the same amount of reagent was used for the shell as for the initial core. This increase in size corresponds to an increase in volume by a factor of 2, indicating that all of the added monomer had grown on the existing core nanoparticles and no new nucleation had occurred. The size distribution is the same in absolute value but because of the increased size it appears like it has narrowed. In this case the effective ligand ratio is also lowered after the addition of the shell monomer, making it possible to form larger nanoparticles. To determine the effect of the undoped core around the nanoparticles, the quantum yields of Ce^{3+}- and Tb^{3+}-doped nanoparticles were determined by comparing the emission intensity with the emission intensity of quinine bisulfate. Upon excitation of the Ce^{3+} absorption band at 282 nm, one emission band of Ce^{3+} at 350 nm and four emission peaks of Tb^{3+} at 489, 543, 584, and 621 nm of the $^5D_4 \rightarrow {}^7F_J$ ($J = 3-6$) were observed (Figure S2, Supporting Information). The quantum yield of the emission was determined by measuring both the emission of Ce^{3+} and the emission of Tb^{3+}. Three methods were used to grow a shell of LaF_3 around the core nanoparticles, which are described in the experimental section and differ only in the way the shell reagents were added to the reaction mixture. Table 2 summarizes the luminescence quantum yields measured by comparing the emission intensity with that of quinine bisulfate.

All methods to synthesize shell material were successful according to the quantum yield measurements. The best method was to grow the shell material around the core by the alternate addition of small portions of the shell reagents. The quantum yield of nanoparticles coated in this way was more than doubled. As a reference experiment, nanoparticles of the same size as the core−shell nanoparticles, but lacking the core−shell structure, were synthesized to check if the increase in quantum yield is not caused by the dilution of the luminescent ions or by the increase in nanoparticle size. Nanoparticles synthesized in this way had a quantum yield of 27%, only a little higher than the core nanoparticles, but clearly much lower than the core−shell nanoparticles. The Ce^{3+} emission in these diluted nanoparticles was stronger compared to the core and the core−shell nanoparticles indicating that energy transfer from Ce^{3+} to Tb^{3+} is less efficient as a result of an increase in the average distance between the Ce^{3+} and Tb^{3+} ions. From this experiment, it can be concluded that the increase in quantum yield is a result of the core−shell structure and not of nanoparticle size or a different distribution of the lanthanide ions in the nanoparticles.

Figure 10 shows the luminescence decay curves of both luminescent levels of the Eu^{3+} ion in LaF_3 nanoparticles, with different equivalents of LaF_3 grown as a shell over the original core using method 3 (see experimental section).

The nonexponential decay of the $^5D_0$ level of the core nanoparticles is clearly observed, and when 1 equiv of shell reagent was grown on the nanoparticles a large change in the decay was observed. A significant increase in the luminescence lifetimes is observed, and the decay deviates much less from single-exponential behavior. The

Table 2. Luminescence Quantum Yields of $(La_{0.4},Ce_{0.45})F_3Tb_{0.15}$ Core−Shell Nanoparticles

nanoparticles	quantum yield[a] (%)
no shell	24
method 1	43
method 2	42
method 3	54
reference[b]	27

[a] The absolute error in the measurements is 2% based on duplicate measurements. [b] In the reference experiment the nanoparticles have the same size as the core−shell nanoparticles, but they lack the core−shell structure.

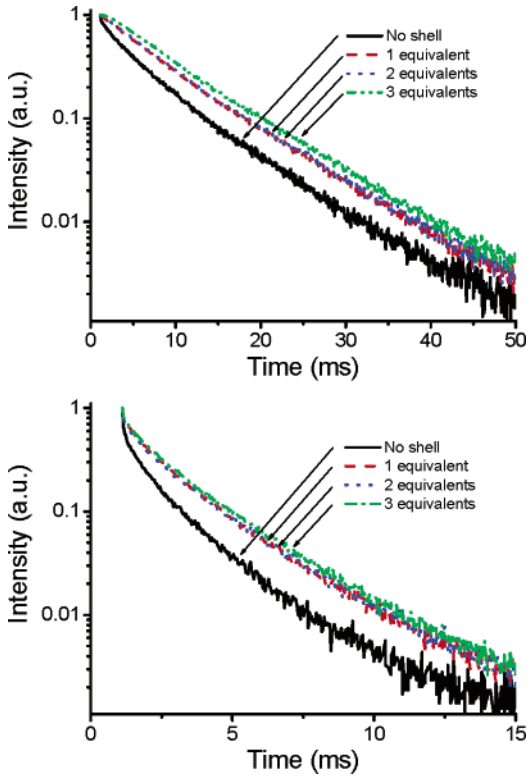

Figure 10. Luminescence decay curves of the $^5D_0$ (top, $\lambda_{ex} = 397$, $\lambda_{em} = 591$ nm) and $^5D_1$ (bottom, $\lambda_{ex} = 397$, $\lambda_{em} = 553$ nm) levels of Eu^{3+} in LaF_3 nanoparticles with a different amount of LaF_3 shell material in toluene.

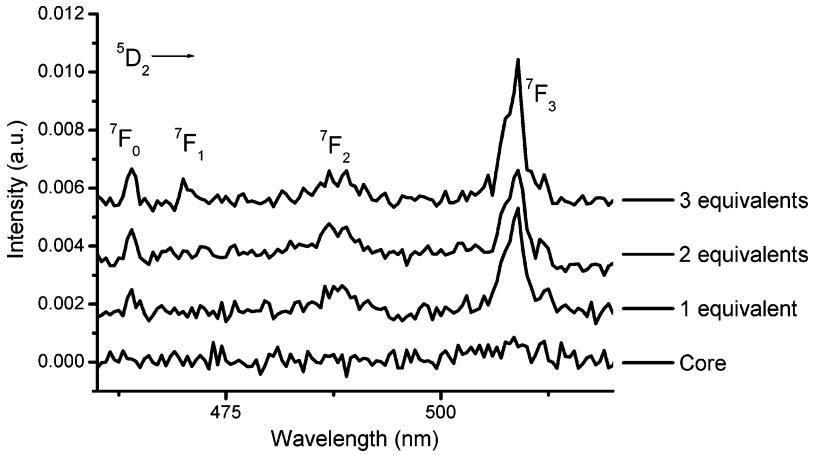

Figure 11. Emission of the $^5D_2$ level of Eu^{3+} in core−shell nanoparticles in dichloromethane (λ_{ex} = 397 nm). The spectra are normalized to the emission of the $^5D_0 \rightarrow {}^7F_1$ emission peak. The offset is for clarity.

Table 3. Luminescence Lifetimes of the $^5D_0$ and $^5D_1$ Levels of LaF_3/Eu Nanoparticles with Different Amounts of LaF_3 Grown over the Original Core, in Toluene[a,b]

	$^5D_0$		$^5D_1$	
	τ_1 (ms)	τ_2 (ms)	τ_1 (ms)	τ_2 (ms)
no shell	7.9 (74%)	3.1 (26%)	2.0 (73%)	0.65 (27%)
1 equiv	9.7 (58%)	5.3 (42%)	2.3 (83%)	0.72 (17%)
2 equiv	9.9 (54%)	5.6 (46%)	2.4 (81%)	0.78 (19%)
3 equiv	9.5 (69%)	5.4 (31%)	2.5 (82%)	0.80 (18%)

[a] The percentages reflect the amount of the component contributing to the total lifetime. [b] The absolute errors in the fit are 0.2 ms in the lifetime and 5% in the component contributing to the total lifetime, based on duplicate measurements.

luminescence lifetimes obtained by fitting with a biexponential decay are shown in Table 3.

The increase in the luminescence lifetimes shows the increased shielding from quenching groups at or near the surface, and the shift in the ratio of the two components of the luminescence lifetime shows that quenching from outside the particle is strongly reduced after the growth of a shell around the core. The biggest change in the decay is observed after the addition of 1 equiv of the shell material. The growth of more shell material has a smaller influence on the decay curve, but with the growth of 3 equiv of LaF_3 over the core, a small rise in the decay curve of the $^5D_0$ level is observed. As a result of the reduced quenching of the higher Eu^{3+} levels such as the $^5D_1$, $^5D_2$, or $^5D_3$ levels, the $^5D_0$ level is populated more slowly in the core−shell nanoparticles, giving rise to a buildup in the luminescence from this level.[15] The values of the lifetimes for 3 equiv of LaF_3 probably deviate from the trend, because fitting of the decay curve was started 5 ms after the excitation pulse. The effect of the shell on the luminescence lifetime of the $^5D_1$ decay is also shown in Figure 10, and the corresponding lifetimes obtained after fitting with a biexponential decay are given in Table 3. The effect is similar to what was observed for the $^5D_0$ level. The growth of 1 equiv of LaF_3 is enough to increase the luminescence lifetime substantially, and a thicker shell only has a small influence on the luminescence lifetime. Luminescence of the $^5D_2$ level of the Eu^{3+} ion located between 460 and 520 nm also becomes visible. The LaF_3/Eu core nanoparticles do not show emission from this level, but in the core−shell nanoparticles emission peaks from this level were visible, as a result of the much reduced quenching. The emission spectra are shown in Figure 11.

After the growth of LaF_3 shell material, emission lines of the $^5D_2 \rightarrow {}^7F_J$ (J = 0−3) transitions start to appear at 464, 472, 489, and 509 nm, respectively. These lines become more intense after the growth of more shell material, indicating reduced quenching of the $^5D_2$ level. In the bulk material, emission from the $^5D_2$ level is also observed at this Eu^{3+} concentration at room temperature.[15]

Conclusions

The solubility of the $LaPO_4$ and LaF_3 nanoparticles can easily be manipulated. The covalent linkage of ligands to the surface of $LaPO_4$ nanoparticles gives the strongest link between particle surface and organic ligand, making it possible to produce very stable nanoparticles that are soluble in organic solvents. The surface of LaF_3 nanoparticles was easily modified by changing the ligands coordinated to the surface, either by using functionalized ligands during the synthesis or by exchanging the ligands after the reaction. The results presented in this paper demonstrate that the synthesis route developed for the synthesis of LaF_3 nanoparticles allows for the synthesis of core−shell structures, in which the core is doped with luminescent lanthanide ions and the shell is not. The luminescence of these core−shell nanoparticles is more efficient than of nanoparticles that lack the shell, because nonradiative processes at or near the surface of the nanoparticles are much reduced. This has been demonstrated by an increase of the quantum yield of (La,Ce)F_3/Tb nanoparticles and by an increase of the luminescence lifetime of the luminescent Eu^{3+} levels of a LaF_3/Eu core after the synthesis of a LaF_3 shell.

Acknowledgment. This research is supported by the Council of Chemical Sciences of The Netherlands Organization for Scientific Research.

Supporting Information Available: TEM picture of LaF_3/Nd nanoparticles synthesized with ligand **2** and emission spectrum of $(La_{0.4}Ce_{0.45})F_3Tb_{0.15}$ nanoparticles in dichloromethane. This material is available free of charge via the Internet at http://pubs.acs.org.

LA048379G